

TRNSYS MODELING OF THE SEGS VI PARABOLIC TROUGH SOLAR ELECTRIC GENERATING SYSTEM

Scott A. Jones
Sandia National Laboratories
PO Box 5800- M/S 0703
Albuquerque, NM 87185

Robert Pitz-Paal, Peter Schwarzboezl
Deutsches Zentrum für Luft- und Raumfahrt e.V.
Linder Höhe
D-51147 Köln, Germany

Nathan Blair
Solar Energy Laboratory
University of Wisconsin
PO Box 5800- M/S 0703
Albuquerque, NM 87185

Robert Cable
KJC Operating Company
University of Wisconsin
PO Box 5800- M/S 0703
Albuquerque, NM 87185

ABSTRACT

A detailed performance model of the 30 MWe SEGS VI parabolic trough plant was created in the TRNSYS simulation environment using the Solar Thermal Electric Component model library. Both solar and power cycle performance were modeled, but natural gas-fired hybrid operation was not. Good agreement between model predictions and plant measurements was found, with errors usually less than 10%, and transient effects such as startup, shutdown, and cloud response were adequately modeled. While the model could be improved, it demonstrates the capability to perform detailed analysis and is useful for such things as evaluating proposed trough storage systems.

TRNSYS AND THE STEC LIBRARY

The TRNSYS simulation environment (Solar Energy Laboratory, 2000) was selected for use in modeling solar thermal power systems for a number of reasons, including modularity, flexibility, and ease of use. Commercially available power cycle modeling codes have many standard components, but frequently limit the user's ability to create new components, tend to be quite expensive, and are not capable of modeling annual performance using weather file data as input. The latest update of TRNSYS, Version 15, was used for this work. It has a number of improvements to the graphical user interface that were found to be very useful.

A library of Solar Thermal Electric Component (STEC) models for both solar and conventional power cycle elements was created for TRNSYS (Pitz-Paal and Jones, 1998). The component models are linked together to form the desired system, thereby permitting flexibility in

modeling different configurations such as standard solar plants or combined fossil-solar (hybrid) designs. The STEC library components are typically detailed steady-state models formulated in thermodynamic quantities such as temperature, pressure, and enthalpy. This high level of modeling detail can be valuable in many cases. For example, the ability of a solar steam generation system to handle startup transients could be analyzed. Of current interest is the evaluation of thermocline storage concepts for trough power plants. To evaluate these concepts, their performance and operational issues associated with startup, shutdown, and cloud transients must be studied on an annual basis.

While annual system performance can be modeled in TRNSYS using these detailed state property components, it is also possible to create less complex component models based on a simple energy balance formulation. This would result in a similar model to SOLERGY (Stoddard et al., 1987), but would be more easily adaptable to different configurations such as hybrid plants. SOLERGY is a public-domain software tool frequently used for annual solar plant performance analysis. The ability in TRNSYS to create and share with others new component and system models also helps provide consistency in modeling efforts undertaken by different organizations around the world, and makes their results more comparable.

Four other parabolic trough power plant models, none in the public domain, should be mentioned. The Luz System Performance Model (Kearney and Gilon, 1988) was used in the design of the SEGS plants and is generally less detailed than the TRNSYS model. KJC Operating Company has improved the Luz model for use in

evaluating plant performance. The FLAGSOL model (Price et al., 1995) is also derived from the Luz model. It has a less detailed simulation of the power cycle than the TRNSYS model and does not provide cycle process data. These models are not modular like the TRNSYS model. The EASY simulation environment was also used for trough plant simulation and will be discussed later.

KJCOC AND THE SEGS PLANTS

KJC Operating Company (KJCOC) operates 5 of the 9 parabolic trough power plants located in the Mojave desert of California (see Figure 1) that have a total rated capacity of 354 MW. KJCOC has many years of experience operating the five 30-MW plants, and has been able to improve peak output and annual performance while reducing operating and maintenance costs over the years (Cohen et al., 1999).

The SEGS VI plant was chosen for modeling because it has been well characterized and there was high confidence in the quality of the data collected. The SEGS plants are permitted (by their power purchase contracts with the local utility) to use natural gas to supply up to 25% of the annual thermal input, but this feature was not included in this first model. One issue is that the SEGS VI plant's operating conditions change in a complicated way in gas fired mode. Additionally, the logic used to determine the amount and timing of fossil burning is dependent upon many factors, is typically evaluated by skilled human judgement, and so is difficult to implement on the computer. Consequently, days with solar-only operation were used for comparison with model predictions.



Figure 1. The 30MW SEGS III-VII parabolic trough plants in the California desert.

THE SEGS VI MODEL

This SEGS VI model differs from a previous Lippke model using the EASY simulation environment (1995) in that publicly available software tools were used and additional complexity was added to more accurately model transient behavior. As will be seen, the steady-state formulation of the models, coupled with the 5-minute time step is sufficient to simulate the plant behavior during the transients studied. Figure 2 shows a schematic of the SEGS VI process flow. Figure 3 shows the TRNSYS user

interface with the SEGS VI model. TRNSYS has the capability to display only part of the system model by assigning components to different, user-definable layers in a similar manner to computer-aided design (CAD) software. Multiple components can also be assigned a single icon called a "macro" to simplify the graphical display, as is the case with the high- and low-pressure turbines and feed water heaters in Figure 3. The lines connecting the components represent the flow of information. For example, the line between the trough field component and the expansion vessel connects the trough field output quantities of temperature and flow rate to the equivalent expansion vessel inputs.

In addition to turning off certain layers of the TRNSYS project shown in Figure 3, some of the connections have been deleted to make the diagram more readable. The methodology for displaying and editing connections in TRNSYS could be improved and made more user friendly. The current methodology results in a very confusing diagram for a complicated system like the SEGS VI model.

1. Parabolic Trough Field

The parabolic trough field model is similar to that of Lippke (1995), and is based on experimental measurements of the SEGS LS-2 trough collector performance (Dudley et al., 1994). The SEGS VI operators manually control the flow rate of the Therminol VP-1 synthetic-oil heat transfer fluid (HTF) through the field of parabolic trough collectors. Normally, they adjust flow to maintain a roughly constant outlet field temperature, and this behavior was modeled. The required mass flow rate of HTF to achieve a user-defined outlet temperature T_{out} is calculated from a first-law energy balance on the field

$$\dot{M} = \frac{\dot{Q}_{net}}{c_p(T_{out} - T_{in})} \quad (1)$$

where,

$$\dot{Q}_{net} = \dot{Q}_{abs} - \dot{Q}_{pipe} \quad (2)$$

and the absorbed power is described by

$$\dot{Q}_{abs} = I \cdot A_{aperture} \cdot \left[LMS(A + B/2(\Delta T_i + \Delta T_o)) + \frac{C(\Delta T_i + \Delta T_o)}{2I} + D \frac{(\Delta T_i - \Delta T_o)^3}{2I(\Delta T_i + \Delta T_o)} \right] \quad (3)$$

The coefficients A, B, C and D are empirical factors describing the performance of the collector. The factor L is the incident angle modifier, M considers end losses and S considers shading of parallel rows. Evaluation of these parameters is described by Lippke (1995). ΔT_i and ΔT_o are the differences between collector inlet and outlet temperature and ambient temperature, and I is the direct normal isolation. \dot{Q}_{pipe} accounts for losses in the piping.

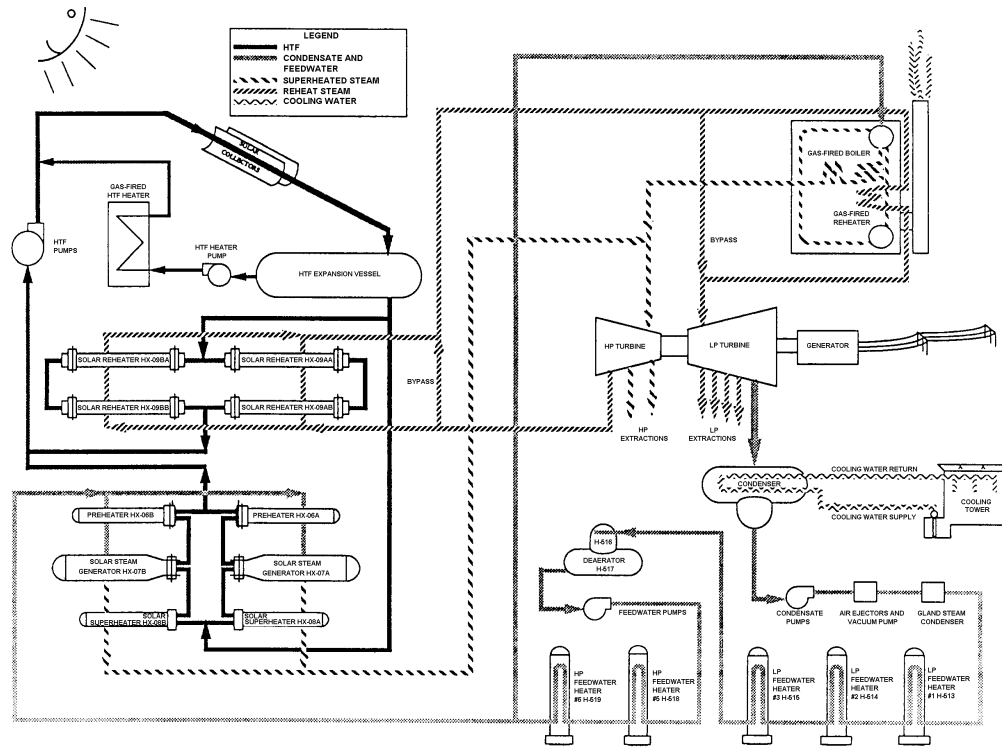


Figure 2. Schematic of the SEGS VI plant.

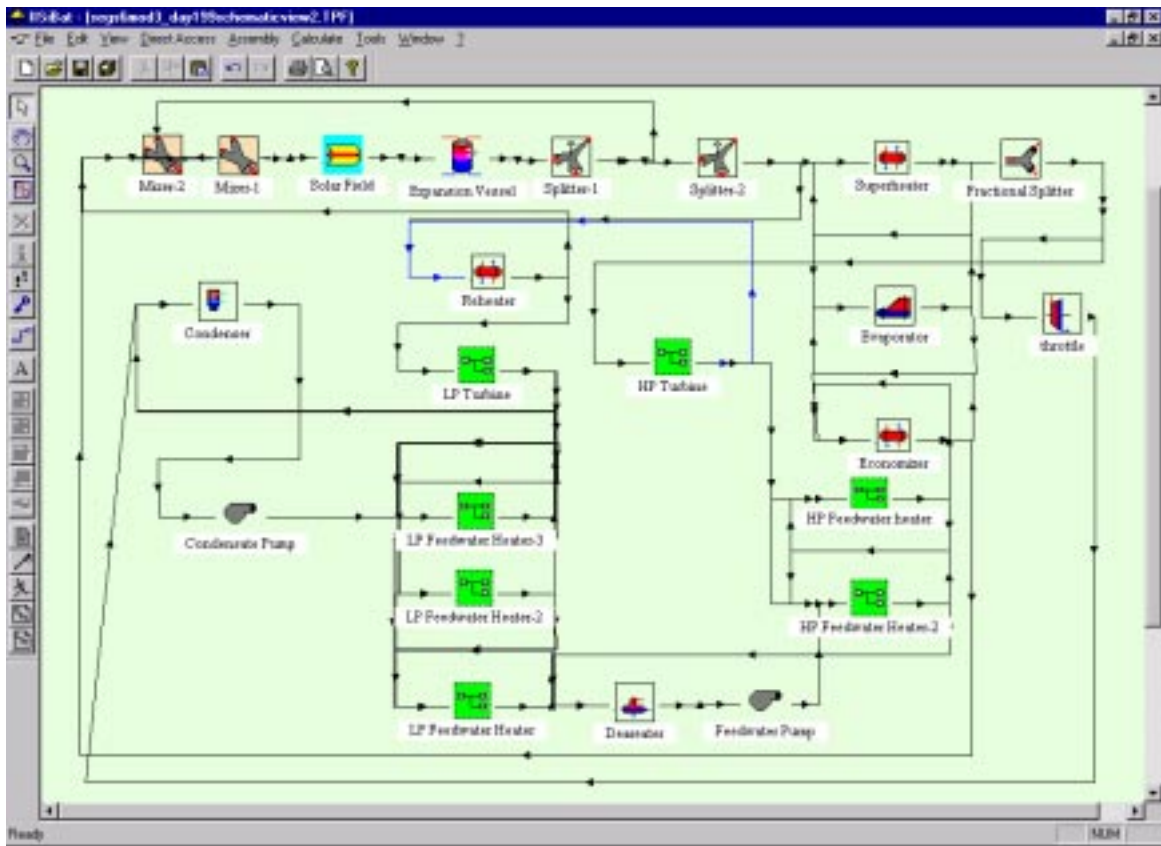


Figure 3. The SEGS VI TRNSYS model.

When the SEGS VI plant is shut down overnight, the steam generation system is “bottled-up,” locking the warm HTF inside. The next time the solar field is operated, the HTF is re-circulated through the field via a bypass loop until its temperature rises to the level of the oil stored in the steam generation system—a value that varies with seasonal and daily weather and is influenced by gas-fired operation. In the model, when the field outlet temperature exceeds 260°C (500°F), a typical value for solar-only operation, flow is directed to the steam generation system and steam production starts.

The HTF undergoes significant volume changes over a day due to changing average temperature. To accommodate this effect at SEGS VI, an expansion vessel is located between the field and the steam generation system. A “Type 4” storage tank component, part of the standard TRNSYS library (Solar Energy Laboratory, 2000), is used to model the expansion vessel.

2. Steam Generation System

The evaporator generates saturated steam and demands feed water flow from the feed water pump. The single-phase economizer, superheater and reheater models use inlet conditions of temperature, pressure, and flow rate of the hot and cold side as input quantities to the model. The transferred heat is evaluated using the effectiveness method in both cases. The overall heat transfer coefficient UA can be scaled with the cold side mass flow rate using a power law. Also, the reference pressure loss may be scaled using a power law with the cold-side flow rate.

3. Turbine

SEGS VI has both high- and low-pressure turbine stages, with reheat of the steam occurring between the stages. Each turbine stage model is assembled using two generic sub-models: one for a turbine stage and one for the steam extraction. The turbine stage evaluates the enthalpy at the stage outlet from the inlet conditions using an inner turbine efficiency that can be specified by the user as a function of the flow rate with a third order polynomial. The pressure at the turbine inlet is evaluated from the pressure at the outlet using Stoidola's law. Mechanical losses are incorporated with a coefficient of mechanical efficiency. The turbine extraction works as an adjustable splitter that receives a flow demand signal, normally from a feed water heater.

To better model turbine startup and shutdown transients, a turbine controller and a bypass loop were added. An approach based on the go/no-go strategy in SOLERGY (Stoddard et al., 1987) was used to define turbine ramp up and synchronization delays for hot, warm, and cold starts. A turbine ramp down period was added to approximate the operator's ability to extend operation by carefully balancing the two competing requirements of steam superheat and minimum pressure. The real turbine

operational limitations of a minimum 16.2 bar (235 psi) steam pressure and 22.2°C (40°F) superheat are imposed. When these conditions are not met, steam is diverted around the turbine to the condenser via a bypass circuit and fractional splitter. During startup or shutdown, the fraction sent to the turbine varies linearly between zero and one over the ramp period. A throttling valve in the bypass loop provides the equivalent pressure drop as the turbine would provide under the same conditions.

4. Feed Water Heaters

The feed water heaters are heat exchangers that condense steam extracted from the turbine to heat feed water before it enters the economizer, thereby increasing the Rankine cycle efficiency. Two TRNSYS components were used to model the feed water heaters, the preheater and the subcooler. The preheater model assumes water of constant heat capacity on the cold side and condensing steam on the hot side. It determines the required steam mass flow rate that would keep the water level in the heat exchanger constant using the effectiveness method to calculate heat transfer. The subcooler is a simple 1-phase heat exchanger based on the standard TRNSYS “Type 5” component with the added ability to scale the overall heat transfer as a function of the cold side flow rate.

5. Deaerator

The deaerator is a type of feed water heater where steam is mixed with subcooled condensate to produce saturated water at the outlet. This helps purge oxygen from the feed water, controlling corrosion. Conservation of energy and mass are used to calculate the required steam flow rate from a turbine extraction to achieve this process.

6. Condenser

Steam exiting the turbine is condensed so that it can be pumped through the steam generation system. Additionally, condensed extraction steam exiting from the feed water heaters is directed to the condenser to be reused. The condenser model assumes a constant temperature difference between the condensate and the cooling water as well as a constant rise in cooling water temperature. Therefore, the condensing pressure depends only on the condensate inlet temperature.

RESULTS

The goal was to create a detailed model that accurately predicted SEGS VI plant behavior on short time scales (i.e. minutes) and through transients. Consequently, the TRNSYS model predictions are compared here with measured plant data on a daily, rather than monthly or annual basis. Results are shown for sunny and cloudy days in 1991 with solar-only operation. Figures 4 and 5 show the weather conditions at KJC on July 18, 1991 and September 19, 1991.

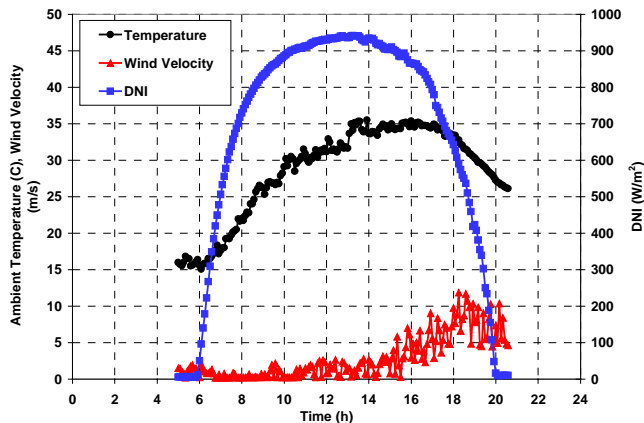


Figure 4. Weather conditions on 7/18/91.

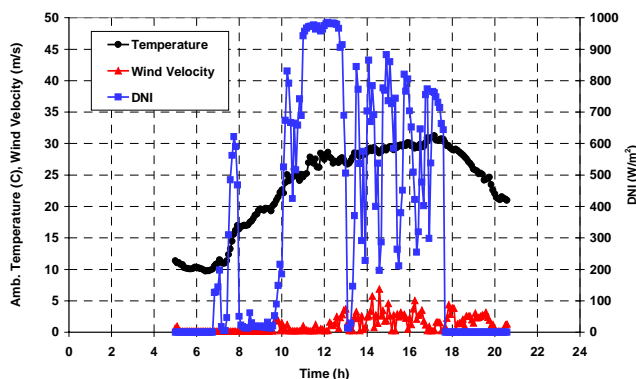


Figure 5. Weather conditions on 9/19/91.

The solar collection results are presented first, followed by the power cycle results. Figures 6 and 7 show the measured and predicted HTF temperatures for the two days at both the inlet and outlet of the trough field. At SEGS VI, the operators manually control the HTF flow rate to achieve the desired field outlet temperature, leading to the slight variations during steady-state seen in the figures. The model uses feedback to exactly achieve the set point temperature of 38°C for 7/18/91 and 375°C for 9/19/91 when sufficient incident power exists. The good match between measured and predicted outlet temperatures indicates this approach is sufficient to model the operator behavior both in sunny and cloudy conditions. The temporal mismatch in outlet temperatures seen in Figure 6 suggests the thermal capacitance of the system is not precisely modeled. The slight mismatch on the cloudy day is likely due to the same phenomenon, but also could result from the DNI measurement being taken at 1-2 discrete locations while the field covers a wide area (because clouds could affect the two differently). The early morning HTF temperatures assumed in the model are closer to measured values on 7/18/91 than on 9/19/91.

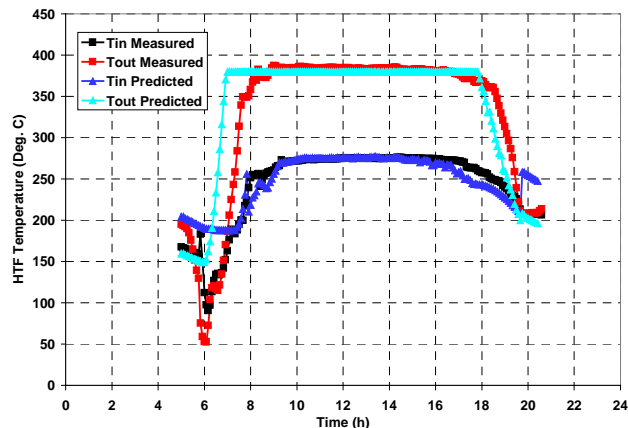


Figure 6. Measured and predicted HTF temperatures at the inlet and outlet of the trough field on 7/18/91.

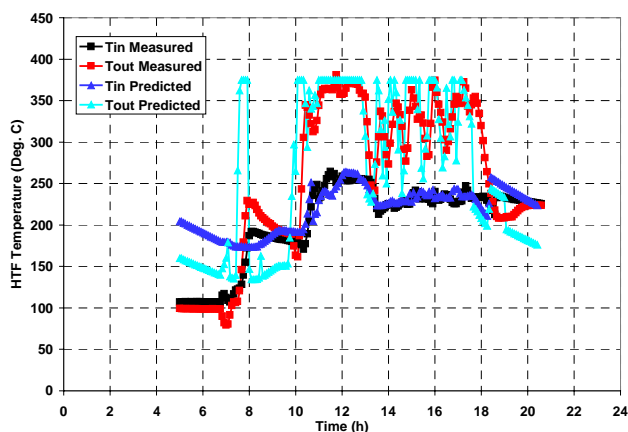


Figure 7. Measured and predicted HTF temperatures at the inlet and outlet of the trough field on 9/19/91.

Figures 8 and 9 show overall good agreement between the measured and predicted HTF flow rates for both days. On both mornings (around 8:00 on 7/18/91 and 10:30 on 9/19/91), the operators increased the HTF flow rate during startup more than the model predicted. This special operational approach permits the starting the turbine more quickly by building steam pressure first, then achieving the required superheat. The turbines at SEGS VI and VII benefit from this special procedure, while the SEGS III-V plants do not need such careful operation during startup.

The current plant operating procedure of maintaining a minimum HTF flow rate of 144,000 kg/hr at all times is modeled, but this operating procedure was not always used in 1991. The higher measured flow rate from 7:00 to 8:00 on 9/19/91 was due to the operators aggressively pursuing energy collection. The model increased HTF flow above the minimum value for only a few minutes before 8:00, when absorbed energy was predicted to exceed losses. The operators are able to view the sky and better estimate the

future weather than the model, which only uses the current time step's values. It appears in this case, the weather did not respond as the operators hoped, and they had to delay solar collection until later.

Shifting to the power cycle, we see in Figures 10 through 13 the measured and predicted steam temperature and steam pressure at the inlet and outlet of the high-pressure turbine for the two days studied. Generally, there is good agreement between measured and predicted values. In particular, the predicted values appear to accurately model the timing.

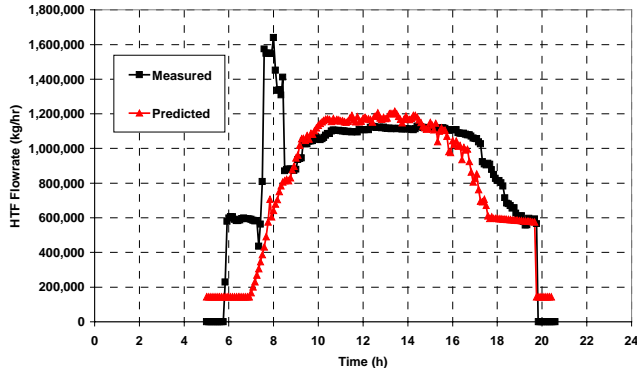


Figure 8. Measured and predicted HTF flow rate on 7/18/91.

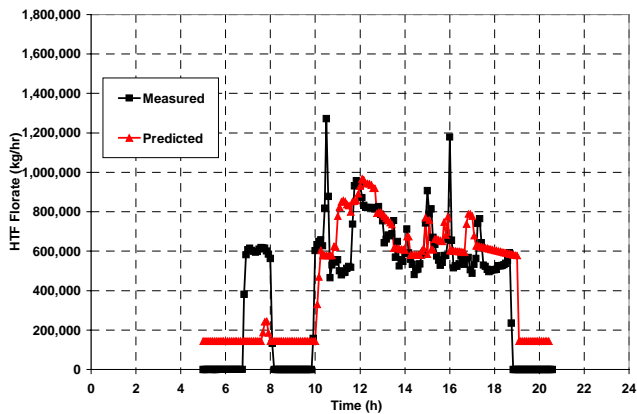


Figure 9. Measured and predicted HTF flow rate on 9/19/91.

Figure 10 shows that the steam outlet pressures generally match predictions on the clear day, but the predicted inlet pressures are about 8 bar (10%) below measured values. The drop in inlet pressure at 8:20 corresponds with the synchronization of the turbine to the grid, and the production of electricity. While still far above the minimum 16.2 bar pressure required for operation, the turbine synchronization is predicted to occur at a substantial 17 bar lower than measured. Furthermore, the predicted drop in pressure after synchronizing the

turbine is larger than was measured. This is due to the special operating procedure discussed previously, where the operators increase HTF flow to build steam pressure before starting the turbine. Figure 11 shows the steam pressures on 9/19/91, where predictions closely match estimates, even during the turbine synchronization. It appears that both startup and steady turbine behavior is well modeled at part-load on 9/19/91, but requires some adjustment for full-load conditions on 7/18/91. Revised and potentially more complicated startup criteria may be needed.

On 7/18/91, the predicted temperatures (Figure 12) are about 15-30°C above measured values at both the beginning and end of the day. On 9/19/91 with intermittent clouds (Figure 13), the predicted turbine outlet temperatures are about 30°C higher than measured, while the inlet temperature predictions are about 10-15°C high. It appears both the pressure loss and inner efficiency equations would benefit from more tuning based on many operating conditions. The low-pressure turbine results are not shown in the interest of brevity.

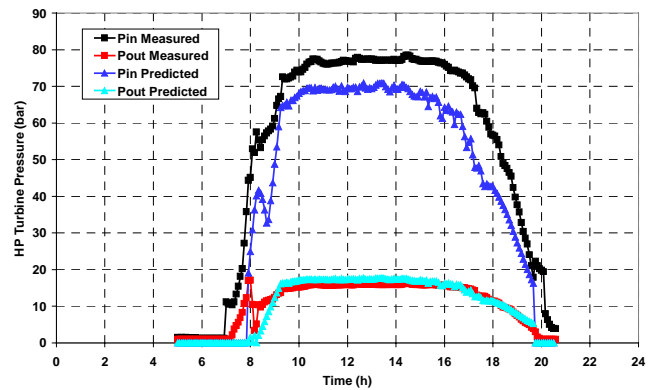


Figure 10. Measured and predicted steam pressures in the high pressure turbine on 7/18/91.

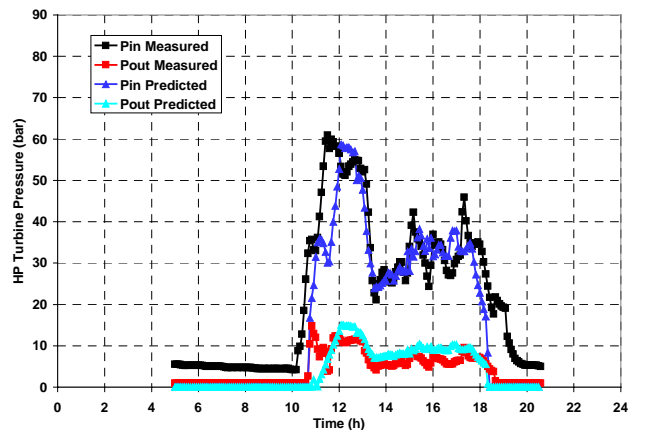


Figure 11. Measured and predicted steam pressures in the high pressure turbine on 9/19/91.

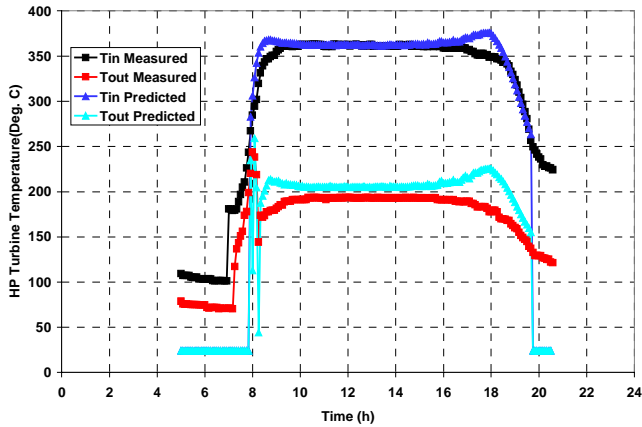


Figure 12. Measured and predicted steam temperatures in the high pressure turbine on 7/18/91.

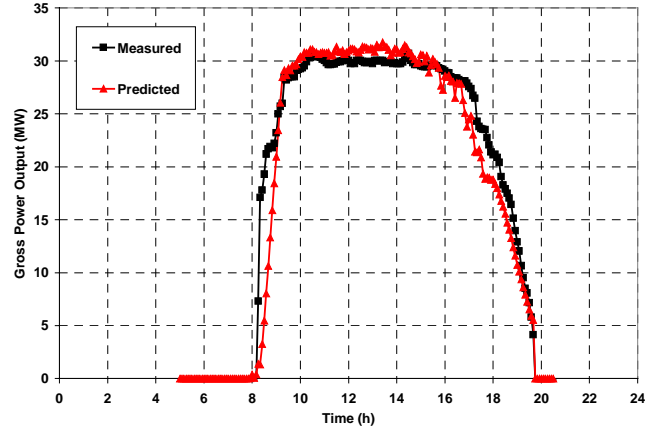


Figure 14. Measured and predicted gross power output on 7/18/91.

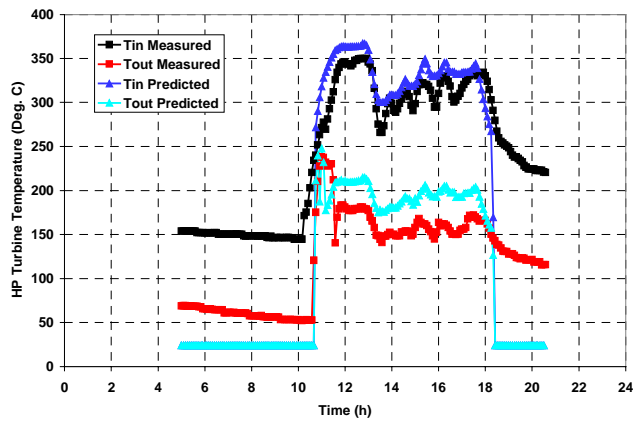


Figure 13. Measured and predicted steam temperatures in the high pressure turbine on 9/19/91.

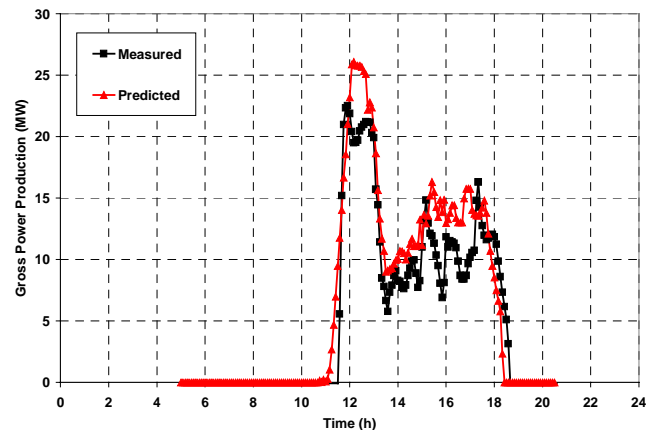


Figure 15. Measured and predicted gross power output on 9/19/91.

Figures 14 and 15 show the gross power output results and Figures 16 and 17 show the parasitic power results for both days studied. On 7/18/91, the gross power predictions closely match measured values, while there is an over prediction on 9/18/91. The opposite trend is seen with plant parasitic power, where the prediction on the sunny day (7/18/91) differs substantially from the measured values, while there is good agreement on the day with intermittent clouds (9/19/91). Figures 18 and 19 summarize the daily total results from the previous 4 figures, and illustrate this effect clearly. Tuning the turbine model to get better temperature and pressure predictions should also improve the accuracy of gross power production predictions.

As seen in Figure 16, the clear day parasitic power predictions match well in the morning, but have greater error in the afternoon when the ambient temperature is higher. Further work is needed to determine if this is causation, or simply correlation.

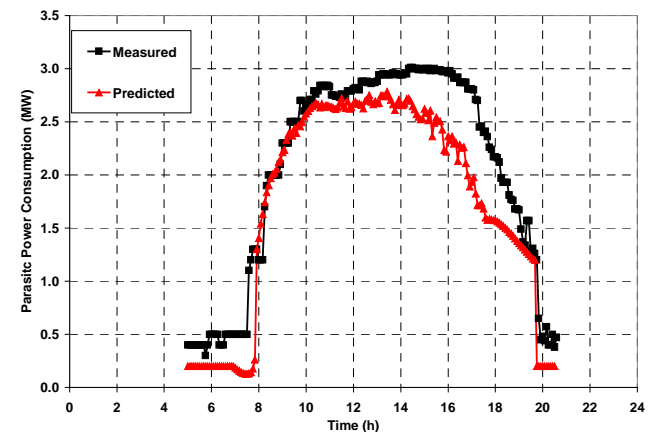


Figure 16. Measured and predicted parasitic power use on 7/18/91.

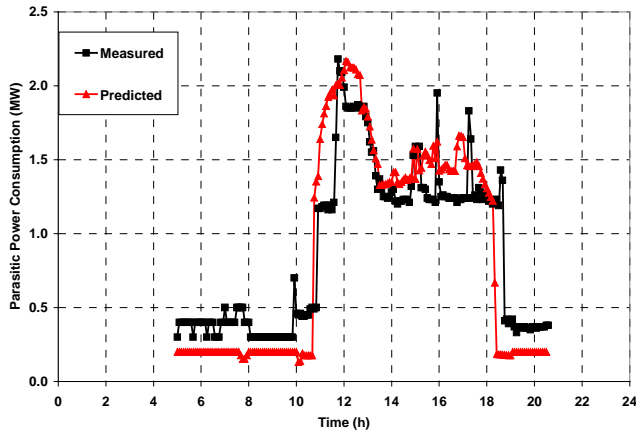


Figure 17. Measured and predicted parasitic power use on 9/19/91.

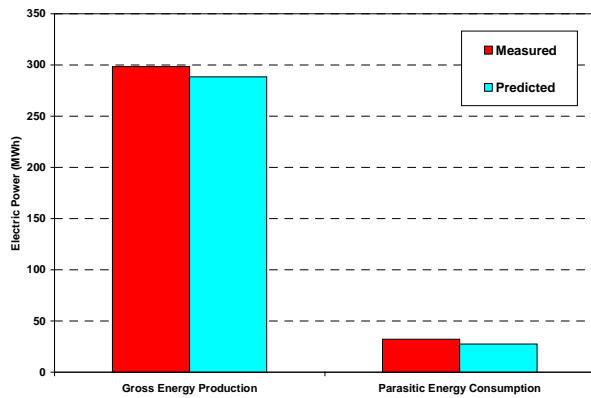


Figure 18. Measured and predicted daily energy totals for 7/18/91.

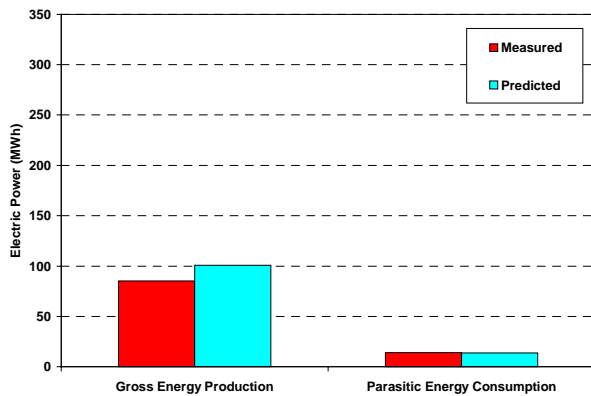


Figure 19. Measured and predicted daily energy totals for 9/19/91.

CONCLUSIONS

The model provides detailed state-property predictions for both the solar field and the conventional power cycle at the SEGS VI plant during solar-only operation. There was

good agreement, usually less than 10% difference, between the model predictions and plant data for both a clear day and for a day with intermittent clouds. Some predictions matched better on the sunny day, while others were better on the cloudy day. Further tuning, particularly of the turbine model, should improve accuracy. Adding thermal capacitance to the model and improving operational controls may also increase accuracy. However, the model already demonstrates that it provides thermodynamic property information with reasonably good accuracy, as is sometimes required for detailed systems analysis. For example, this model could be used as the basis for evaluating the annual performance and operational issues of proposed trough thermochemical storage concepts, including the effects of startup, shutdown, and cloud transients.

ACKNOWLEDGEMENTS

Sandia National Laboratories is a multi-program laboratory operated by Sandia Corporation, a Lockheed Martin Company, for the United States Department of Energy under Contract DE-AC04-94AL85000.

REFERENCES

- Cohen, G.E., Kearney, D.W., Kolb, G.J., 1999, "Final Report on the Operation and Maintenance Improvement Program for Concentrating Solar Power Plants," SAND99-1290, Sandia National Laboratories, Albuquerque, NM.
- Dudley, V.E., Kolb, G.J., Mahoney, A.R., Mancini, T.R., Matthews, C.W., Sloan, M., Kearney, D., 1984, "Test Results SEGS LS-2 Solar Collector," SAND94-1884, Sandia National Laboratories, Albuquerque, NM.
- Kearney, D. and Gilon, Y., 1988, "Design and Operation of the Luz Parabolic Trough Solar Electric Plants," VDI Berichte NR. 704, Cologne, Germany.
- Lippke, F., 1995, "Simulation of the Part-Load Behavior of a 30 MWe SEGS Plant," SAND95-1293, Sandia National Laboratories, Albuquerque, NM.
- Pitz-Paal, R., and Jones, S.A., 1998, "A TRNSYS Model Library for Solar Thermal Electric Components (STEC)," A Reference Manual, Release 1.0, IEA-Solar Power and Chemical Energy Systems, Task III: Solar Technologies and Applications.
- Price, H.W., Svoboda, P., Kearney, D., 1995, "Validation of the FLAGSOL Parabolic Trough Solar Power Plant Performance Model," Solar Engineering 1995, American Society of Mechanical, Maui, Hawaii.
- Solar Energy Laboratory, 2000, "TRNSYS, A Transient Simulation Program," University of Wisconsin, Madison, <http://sel.me.wisc.edu/trnsys/>.
- Stoddard, M.C., Faas, S.E., Chiang, C. J. and Dirks, A.J., 1987, "SOLERGY - A Computer Code for Calculating the Annual Energy from Central Receiver Power Plants," SAND86-8060, Sandia National Laboratories, Livermore, CA.